



Article

Enhanced Moisture Management in Textiles via Spray-Coated Water-Based Polyhydroxyalkanoate Dispersions

Marta A. Teixeira ^{1,*}, Wael Almustafa ², Joana Castro ¹, Catarina Guise ¹, Helena Vilaça ¹ and Carla J. Silva ¹

- CITEVE-Technological Center for the Textile and Clothing Industries of Portugal, 4760-034 Vila Nova de Famalicão, Portugal; jcastro@citeve.pt (J.C.); cguise@citeve.pt (C.G.); hvilaca@citeve.pt (H.V.); cjsilva@citeve.pt (C.J.S.)
- Department of Applied Logistics and Polymer Sciences, Kaiserslautern University of Applied Science, Schoenstraße 11, 67659 Kaiserslautern, Germany
- * Correspondence: mteixeira@citeve.pt

Abstract

Developing sustainable textile finishes that enhance moisture management and breathability remains a significant challenge in designing high-performance apparel. In this study, we propose an eco-friendly coating strategy utilizing an aqueous dispersion of poly(3hydroxybutyrate)-diol (PHB.E.0), a member of the polyhydroxyalkanoate (PHA) family. This coating was applied to woven polyester (PES) and cotton (CO) fabrics using a lowimpact spray-coating technique, aiming to improve functional properties while maintaining environmental sustainability. This solvent-free process significantly reduces chemical usage and energy demand, aligning with sustainable manufacturing goals. Successful deposition of the coating was confirmed by scanning electron microscopy (SEM), attenuated total reflectance Fourier-transform infrared spectroscopy (ATR-FTIR), elemental (C/O) analysis, and thermogravimetric analysis (TGA), which also revealed substrate-dependent thermal behaviour. Wettability, water absorption, and permeability tests showed that the coated fabrics retained their hydrophilic character. PHB.E.0 coatings led to a significant reduction in air permeability, particularly after hot pressing at 180 °C, from ≈670 to \approx 171 L·m⁻² s⁻¹ for PES and from \approx 50 to \approx 30 L·m⁻²·s⁻¹ for CO, without compromising water vapor permeability. All coated samples maintained high breathability, essential for wearer comfort. These results demonstrate that PHB.E.0 coatings enhance wind resistance while preserving moisture vapor transport, offering a sustainable and effective solution for functional sportswear.

Keywords: Polyhydroxyalkanoate (PHA); modified PHA; PHB.E.0; biodegradable coating; aqueous dispersion; PHA-spray coating; wind resistance



Academic Editor: Jiri Militky

Received: 17 September 2025 Revised: 14 October 2025 Accepted: 19 October 2025 Published: 23 October 2025

Citation: Teixeira, M.A.; Almustafa, W.; Castro, J.; Guise, C.; Vilaça, H.; Silva, C.J. Enhanced Moisture Management in Textiles via Spray-Coated Water-Based Polyhydroxyalkanoate Dispersions. Coatings 2025, 15, 1237. https://doi.org/10.3390/coatings15111237

Copyright: © 2025 by the authors. Licensee MDPI, Basel, Switzerland. This article is an open access article distributed under the terms and conditions of the Creative Commons Attribution (CC BY) license (https://creativecommons.org/licenses/by/4.0/).

1. Introduction

In recent years, advancements in textile materials have introduced new functional properties to clothing, enhancing their performance for the wearer, particularly in terms of comfort. This encompasses both sensory comfort (touch and feel) and thermophysiological comfort, which involves the body's thermal regulation and moisture management, in accordance with established comfort standards [1]. Comfort is generally defined as a state of psychological, physiological, and physical well-being resulting from an optimal interaction between the human body and its environment. In clothing science, comfort encompasses several dimensions, including thermophysiological, psychological, ergonomic, and sensory aspects. Thermophysiological comfort refers to the effective regulation of heat and

Coatings 2025, 15, 1237 2 of 18

moisture transfer from the skin to the surrounding environment, ensuring the maintenance of core body temperature within the optimal range of 36.5–37.5 °C [2]. Therefore, this definition highlights the critical role of textile breathability, particularly parameters such as air and water vapor permeability, in ensuring clothing comfort [3]. In recent decades, researchers worldwide have focused on developing innovative wearable textile systems to meet human comfort needs more efficiently. The textile comfort has been explored through various strategies, including fibre microstructuring, the use of hydrophilic-hydrophobic fibre combinations, particular fabric constructions, and surface modification, including laminations, coatings, and chemical treatments [2,4]. Among various strategies, surface modifications stand out as one of the most straightforward and effective approaches for tailoring textile properties to enhance wearer comfort. These techniques enable precise adjustment of fabric characteristics without compromising the inherent qualities of the textile substrate [5]. Current commercial applications illustrate the success of such modifications, prominently featuring advanced microfibre polyester fabrics treated with silicone or fluorinated compounds for water repellency [6]. Innovative microporous coatings and membranes have also revolutionized performance textiles, with notable examples including Gore-Tex[®], which utilizes microporous polytetrafluoroethylene (PTFE) membranes, and Aquatex[®], based on polyurethane coatings. Additionally, hydrophilic solid coatings and films, such as Sympatex[®], derived from modified polyester films, provide alternative mechanisms for moisture management and breathability [7,8]. Collectively, these technologies highlight the pivotal role of surface modification in advancing functional textiles geared toward enhanced user comfort and performance.

However, despite their functional advantages, the extensive use of fluorinated polymers, polyurethanes, and silicones in textile surface treatments presents significant environmental challenges [9,10]. Fluorinated compounds, including PTFE-based materials, are exceptionally persistent due to the strength of their carbon-fluorine bonds, rendering them resistant to natural degradation processes [11]. Consequently, these substances accumulate in ecosystems and living organisms, leading to long-term toxicological risks for wildlife and human health, especially due to bioaccumulation and widespread environmental distribution [12]. Similarly, polyurethanes and silicones, though less chemically stable and durable, are largely non-biodegradable and complicate waste management. Their degradation contributes to microplastic pollution, a growing concern, given that synthetic textile fibres represent a major source of microplastics in aquatic environments. This persistence and environmental impact underscore the urgent need to develop sustainable, eco-friendly alternatives in textile surface engineering, solutions that maintain high performance while minimizing ecological harm [13,14]. In this context, polyhydroxyalkanoates (PHAs) emerge as a promising class of biodegradable polymers capable of replacing petroleum-derived materials in textile applications. PHAs are naturally produced thermoplastic polyesters synthesized by bacteria, capable of degrading in diverse environmental conditions without generating persistent pollutants [15]. Their production avoids the use of volatile organic solvents, making them inherently safer and more sustainable. Importantly, their material properties can be precisely tailored by adjusting the ratio and composition of copolymers, enabling performance customization for specific applications [16].

PHAs have also demonstrated commercial viability in the packaging industry, where PHA-based coatings are being developed for paperboard and paper substrates to impart essential barrier properties, such as water resistance, oil repellency, and mechanical strength, without compromising compostability [17,18]. This broader adoption underscores the material's versatility and strong alignment with circular economic principles. Additionally, PHAs offer innovative end-of-life options, including conversion into fertilizers or fermentation feedstocks to produce new polymers [19]. The integration of PHAs into

Coatings 2025, 15, 1237 3 of 18

textile surface engineering therefore represents a viable, forward-thinking approach toward high-performance and environmentally responsible materials that deliver both functional benefits and ecological sustainability [20]. While PHAs have recently been introduced as coatings for yarns and fabrics using conventional methods such as extrusion and doctor blade application [21], their potential for direct deposition onto textile surfaces via spray coating techniques remains largely underexplored. To the best of our knowledge, this study is the first to employ a spray coating system to apply an aqueous, chemically modified PHA dispersion onto two distinct fabric substrates, polyester (PES) and cotton (CO).

The spray coating technique enables precise control over both the quantity and uniformity of polymer deposition, ensuring consistent surface coverage while preserving the intrinsic properties of the textile substrates. This method offers several advantages, including scalability, cost-effectiveness, and compatibility with existing industrial textile finishing processes, making it a promising approach for large-scale implementation [22].

By optimizing parameters such as spray pressure, polymer concentration, and drying/curing conditions, durable and functional PHA coatings were achieved, providing enhanced surface characteristics without compromising the fabric's breathability or mechanical integrity. This approach highlights a practical pathway to integrate biodegradable polymer coatings into conventional textile manufacturing, advancing the development of sustainable, high-performance materials.

Building on these advances, this study reports the development and application of aqueous, solvent-free PHA dispersions specifically formulated for textile substrates. By incorporating surfactants and dispersants, the coating process achieved uniform and consistent deposition while ensuring polymer stability within the dispersions. The functional properties of the coated textiles were comprehensively evaluated, underscoring the promise of PHA coatings as sustainable alternatives for textile surface engineering. This work marks a pivotal step toward the industrial adoption of biodegradable polymer coatings, addressing urgent environmental challenges without compromising the intrinsic functionality of the materials.

2. Materials and Methods

2.1. Materials and Reagents

Poly(3-hydroxybutyrate) (P3HB) with a weight average molecular weight Mw = 250,000 g·mol $^{-1}$ and a polydispersity index (PDI) = 2.7 was purchased from Biomer (Schwalbach/Germany). Ethylene glycol (\geq 99%) and p-toluene sulfonic (\geq 99%) acid were purchased from Sigma Aldrich (Darmstadt, Germany). The PHB.E.0 powder is a P3HB diol (Mw 24,000 Da, PDI 1.83) characterized by a particle size distribution ranging from \leq 45 μ m to \geq 250 μ m. Woven 100% polyester fabrics (PES, 235 g·m $^{-2}$) pretreated for printing and woven 99% cotton, and 1% elastane fabrics (CO, 369 g·m $^{-2}$) were kindly provided by Riopele (V.N. Famalicão, Portugal). The surfactants Span $^{\text{(B}}$ 60, Span $^{\text{(B}}$ 80, Tween $^{\text{(B}}$ 20, and Tween $^{\text{(B}}$ 80 were kindly provided by Croda Iberica SAU (Barcelona, Spain). The surfactant, Sodium dodecyl sulphate (SDS), was acquired from TCI Europe (Zwijndrecht, Belgium). The wetting and dispersing additives Disperbyk 190, 193, and 195 were kindly provided by BYK (Wesel, Germany).

2.2. Synthesis of P3HB Diol via Alcoholysis

Ten grams of P3HB was dissolved in 100 mL of chloroform under reflux at $80 ^{\circ}\text{C}$ for one hour. Subsequently, a tenfold molar excess of ethylene glycol (relative to P3HB) was added to the solution, along with 0.5 g of p-toluenesulfonic acid as a catalyst. The mixture was refluxed for an additional four hours. After the reaction, the mixture was poured into ethanol to precipitate the product. The precipitated P3HB-diol was washed with ethanol

Coatings 2025, 15, 1237 4 of 18

and filtered. The resulting P3HB-diol (PHB.E.0) was then dried under vacuum at $40\,^{\circ}\text{C}$ to constant weight. The Mw and the PDI were determined by gel permeation chromatography (GPC) using an Agilent chromatograph (Waldbronn, Germany), conducted in chloroform, and calibrated with polystyrene standards.

2.3. Coating Aqueous PHB.E.0 Dispersions on Woven Fabrics

Several aqueous dispersions were prepared by dispersing 1–5% w/v PHB.E.0 (particle size \leq 45 µm) in distilled water for 30 min. The polymer particle size was adjusted firstly by sieving using a 250 μm stainless steel vibratory sieve (Retsch GmbH, Haan, Germany), followed by sieving using a 45 μm stainless steel sieve. The pH was then adjusted to neutral using a 5% (w/v) sodium carbonate solution. Following, 0.05–6% w/v Tween 80 and 0.05–6% w/v Disperbyk 190 were added to the PHB.E.0 dispersion and stirred for 1 h. To obtain a uniform dispersion, the solution was sonicated using a Q700 sonicator (QSonica, Newtown, CT, USA) at 65% amplitude, corresponding to a power output of 90-100 W, for durations ranging from 1 to 45 min. The selected dispersion was applied to 16×16 cm samples of polyester and cotton fabrics using an E1850+ Complete Cabinet Standard Model spray system, equipped with a hydraulic nozzle (diameter of 0.28 mm) (AutoJet Technologies, Glendale Heights, IL, USA). The spraying process was carried out at a pressure of 0.4 MPa. The distance between the spray gun and the fabric surface was maintained at 40 cm, and the spray flow rate was set to 100%, corresponding to 67.01 mL⋅min⁻¹. Each sample was sprayed for a duration of 5 s. Following deposition, the coated fabrics were dried at 100 °C for 10 min, then thermofixed at 150 °C for 5 min. Subsequently, a pressing process was performed at 160 and 180 °C for 15 s under a pressure of 5 bar to enhance polymer fixation efficiency.

2.4. Characterization

2.4.1. Dispersion Characterization

The PHB.E.0 dispersion was characterized through two complementary analyses: rheological measurements and particle size and charge determination. The rheological properties were assessed using a Fungilab Smart L (Barcelona, Spain) viscometer equipped with a Low-Consistency Plate (LCP) adapter. Measurements were conducted at 25 $^{\circ}$ C under controlled conditions to ensure reproducibility. The viscosity of the dispersion was recorded as a function of shear rate, with each measurement performed in triplicate.

Particle size distribution and polydispersity were determined using dynamic light scattering (DLS) on a Malvern Zetasizer Nano ZS90 (Malvern Panalytical Ltd., Malvern, Worcs., UK). Samples were diluted firstly with deionized water to avoid multiple scattering effects and equilibrated at 25 $^{\circ}$ C for 10 min before measurement. All measurements were performed in triplicate.

2.4.2. Scanning Electron Microscopy (SEM)

Morphological analyses of the uncoated fabrics and those coated with PHB.E.0 dispersions were performed using a ZEISS EVO 10 Scanning Electron Microscope (Oberkochen, Germany) at an accelerating voltage of 20 kV. Before analysing, PHB.E.0-coated fabrics were coated with a thin layer of Au using a BIO-RAD SC502 sputter coater (Bio-Rad Laboratories, Watford, UK). Images at a magnitude of $500 \times$ were used.

2.4.3. Attenuated Total Reflectance—Fourier Transform Infrared Spectroscopy (ATR-FTIR)

ATR-FTIR spectra were collected in triplicate. A Spectrum One (PerkinElmer, Rodgau, Germany) spectrophotometer with a diamond crystal was used. Each spectrum was obtained in transmittance mode, by accumulation of 45 scans with a resolution of 4 cm $^{-1}$ in the range of 650 and 4000 cm $^{-1}$.

Coatings 2025, 15, 1237 5 of 18

2.4.4. Thickness and Grammage

The thickness of fabrics, both before and after coating, was measured using a thickness gauge (SCHRÖDER Rainbow, Weinheim, Germany). The fabrics were placed between two plates or sensors, and the thickness was displayed digitally to ensure greater precision. The grammage was determined following ISO 3801: 1977—Textiles—Determination of Mass per Unit Length or Mass per Unit Area.

2.4.5. Thermogravimetric Analysis (TGA)

Thermal degradation behaviour was assessed by monitoring the weight loss of the samples over a temperature range of 30 °C to 600 °C at a heating rate of 10 °C·min⁻¹ under a nitrogen flow of 40 mL·min⁻¹. Measurements were conducted using a TGA 4000 instrument (PerkinElmer, Rodgau, Germany) with ceramic pans, and data acquisition was managed via PyrisTM software, Version 11 (PerkinElmer). Results are reported as percentage weight loss versus temperature, and all experiments were performed in triplicate to ensure reproducibility.

2.4.6. Wettability

Water contact angle measurements were performed using a Theta Flex optical tensiometer (Biolin Scientific, Gothenburg, Sweden) coupled with the OneAttension videobased drop shape analyzer software (version 1.2), following the sessile drop method. Droplets of 3 μ L distilled water were gently placed onto the textile surface to ensure direct contact without free fall. Ten measurements were conducted for each sample type, and static contact angles were recorded immediately after the droplets stabilized on the surface.

2.4.7. Water Absorption Test

The water absorption capacities of samples were evaluated according to ISO 20158:2028. Initially, each sample was placed in a moisture analyser (MBT 64M, VWR, Weinheim, Germany) at 35 °C until equilibrium weight was achieved. The difference between the initial and final masses was recorded. To determine the water absorption, each sample was immersed in a beaker containing 400 mL of water. The time each sample remained on the surface before sinking to the bottom of the beaker was recorded, up to a maximum of 180 s. Samples that remained on the surface for more than 180 s were noted as having a sinking time greater than 180 s. Once a sample reached the bottom of the beaker, it was immediately removed, placed in the moisture analyser, and dried at 150 °C. The water absorption capacity was calculated by the difference between the dried and wet masses of the sample. For samples that did not sink and remained on the surface for longer than 180 s, they were carefully submerged to the bottom of the beaker using tweezers. After reaching the bottom, the samples were immediately removed, placed in the moisture analyser, and dried at 150 °C. The water absorption capacity was again determined by the difference between the dried and wet masses.

2.4.8. Permeabilities

Air and water vapor permeability (WVP) studies were conducted according to standards ISO 9237:1997 and BS 7209:1990, respectively. Air permeability was measured using a Textest FX 3300 (Textest AG, Schwerzenbach, Switzerland) device under an applied air pressure of 100 Pa, a value commonly used for clothing applications. For each fabric, three samples were tested, with measurements taken at nine equidistant points (20 cm² each) distributed transversely across the fabric surface. On the WVP assessment, a water vapour permeability tester (M261, SDL Atlas, Rock Hill, SC, USA) was used. The samples were placed over cylindrical cups containing 46 mL of deionized water (dH₂O) for 16 h,

Coatings 2025, 15, 1237 6 of 18

with the coated side of the fabric-oriented outward, representing the exterior side of the clothing. Water evaporation through the textile substrates was evaluated by weighing the test cups before and after the exposure period. Experiments were conducted at room temperature (20–24 $^{\circ}$ C) and 65% relative humidity (RH). An open cup covered with a reference substrate served as the control. All measurements were performed in triplicate. The water vapor transmission rate (WVTR) and the WVP index (I) were calculated using the following equations:

$$WVTR = 24\Delta W/A\Delta t \tag{1}$$

$$I = WVPs/WVPr \times 100$$
 (2)

where ΔW is the difference in the water weight (g) before and after the 16 h test, A is the inner area of the cup (mm), Δt is the exposure time (h), WVPs is the WVP of the samples, and WVPr is the WVP of the reference.

3. Results and Discussion

3.1. Process Optimization of PHA Dispersion Preparation and Spray Coating on Textiles

A spray-coating approach was adopted as an alternative finishing method using P3HB-diol (PHB.E.0), a chemically modified form of P3HB containing hydroxyl groups. The modified polymer exhibited a Mw of 24,204 and a PDI of 1.7, which facilitated the preparation of stable water-based dispersions, enabling environmentally friendly and easily processable formulations. To ensure consistent and clog-free application, a stable, low-concentration aqueous dispersion of PHB.E.0 was developed. Due to the inherent hydrophobicity of the polymer, key formulation parameters—including polymer particle size, concentration, surfactant and dispersant type and concentration, and stirring and sonication times were systematically optimized. Distilled water was chosen as the dispersing medium for its environmental benefits, in line with the European Union project, and because the spray system is incompatible with solvents that may corrode components or pose safety risks. The system's maximum allowable viscosity is 280 cP, necessitating precise control of formulation parameters.

A systematic optimization process was conducted to develop stable and sprayable PHB.E.0 dispersions. Formulations containing PHB.E.0 concentrations between 1% and 5% w/v were prepared and evaluated under varying conditions. Different surfactants (Span® 60, Span® 80, Tween® 20, Tween® 80, SDS) and dispersants (Disperbyk 190, 193, 195) were screened within a concentration range of 0.05–6% w/v, combined with sonication times from 1 to 45 min and polymer particle sizes between \leq 45 μ m and \leq 250 μ m. Through this iterative optimization, the formulation exhibiting the best stability, homogeneity, and suitability for spray application was identified as containing 2% w/v PHB.E.0 (particle size \leq 40 μ m), 6% w/v Tween® 80, and 3% w/v Disperbyk 190. This dispersion exhibited a viscosity of \approx 2 cP with a torque of 31.4%, a particle size of \approx 572 nm with a PDI of \approx 0.2, and a zeta potential of -9.2 ± 18.9 mV (see Section S2 of the Supplementary Information). Despite a low mean zeta potential, the dispersion may be stabilized by steric effects of Tween® 80 and by localized electrostatic repulsion from highly charged particles (SD \pm 18.9 mV).

To achieve uniform spray-coated textiles, a comprehensive evaluation of key spray parameters was conducted, including nozzle type, spray flow rate, spray pressure, nozzle-to-substrate distance, and application duration. Although not yet a standard practice in the textile industry, spray coating is considered a valuable technique due to its potential for scalable and efficient deposition of functional coatings over large surface areas through controlled wet processes [23]. Nozzle selection ultimately favored the hydraulic type, as pneumatic nozzles showed a higher tendency to clog, particularly when spraying hydrophobic polymer dispersions. Among the parameters evaluated, spray pressure was also

Coatings 2025, 15, 1237 7 of 18

found to be critical. Excessive spray pressure generates finer droplets, which increases the likelihood of coating solution penetrating the textile substrate. This can alter the fabric's microstructure and compromise surface functionality, negatively affecting coating uniformity, durability, and the desired performance characteristics [24]. Therefore, precise optimization of spraying parameters is essential to control coating thickness, homogeneity, and fabric integrity, ensuring that the final product meets stringent functional specifications [25].

Based on parameter optimization and the rheological characteristics of the polymer dispersion, a spray pressure of 0.4 MPa was identified as optimal. When combined with an optimized nozzle-to-substrate distance, this pressure maximized surface coverage while minimizing material waste and preventing excessive penetration into the fabric. Specifically, a nozzle-to-fabric distance of 40 cm and a spray duration of 5 s provided the most effective surface modification, reducing polymer dispersion loss and promoting consistent, uniform coating deposition.

To evaluate the necessity of a hot pressing step, two different post-treatment temperatures (160 $^{\circ}$ C and 180 $^{\circ}$ C) were applied to the PHB.E.0-coated fabrics. A control sample, i.e., coated fabrics without any hot pressing step, was also included for comparison.

3.2. Morphological Analysis of Fabrics Coated with PHB.E.0 Dispersions

To confirm and analyse the presence of PHB.E.0 on the textile substrates after the spray process, SEM imaging was performed (Figure 1). The control PES and CO fabrics (images A and D) exhibited smooth surfaces, especially in the PES samples. After applying the polymeric spray finish, distinct particle deposition was clearly visible (images B, C, E and F). These micrographs demonstrate the effectiveness of the coating process, confirming the successful deposition of PHB.E.0 on the fabric surfaces. The coated textiles exhibited a uniform and homogeneous distribution of the polymeric material throughout the fabric matrix, indicating consistent coverage. In samples subjected to hot pressing, the fibres appeared more compacted and flattened (images A1, B1, D1, and E1). At higher magnifications (C and F), PHB.E.0 was observed not only coating the fibre surfaces but also partially penetrating the fabric structure, confirming the polymer's infiltration during the spraycoating process. During hot pressing, the polymer particles on the fibre surfaces partially fuse, forming a continuous coating that adheres closely to the fibres. This fusion accounts for the reduced visibility of individual particles compared to substrates coated without hot pressing. Under these conditions, a continuous polymer film is clearly observable on the fibre surfaces, as exemplified in images C1 and F1.

3.3. ATR-FTIR Analysis

To assess the presence of PHB.E.0 on the fabrics, and to investigate potential interactions between the polymer and the textile substrate, ATR-FTIR was conducted. The FTIR spectra of uncoated fabrics (PES and CO), PHB.E.0 polymer powder, and PHB.E.0-coated fabrics are presented in Figure 2. The spectra clearly reveal the chemical identities of both textile substrates used. The spectrum of the PES substrate (Figure 2a) displays the characteristic absorption bands of aromatic polyester. The most prominent peak appears at 1715 cm $^{-1}$, attributed to the stretching vibration of the ester carbonyl (C=O) group. A strong band at 1243 cm $^{-1}$ corresponds to C–O stretching of the aromatic ester linkage, while the band at 1093 cm $^{-1}$ is associated with C–H in-plane bending of the aromatic ring. Additionally, a band at 723 cm $^{-1}$ indicates aromatic C–H out-of-plane bending, another typical feature of PES [26,27]. The CO substrate (Figure 2b) also exhibits its expected spectral features, confirming the presence of cellulose. Notably, a strong band at 1030 cm $^{-1}$ is assigned to C–O stretching vibrations in the polysaccharide backbone, while the band at 892 cm $^{-1}$ is attributed to the β -glycosidic linkage, a key marker of cellulose structure [28,29].

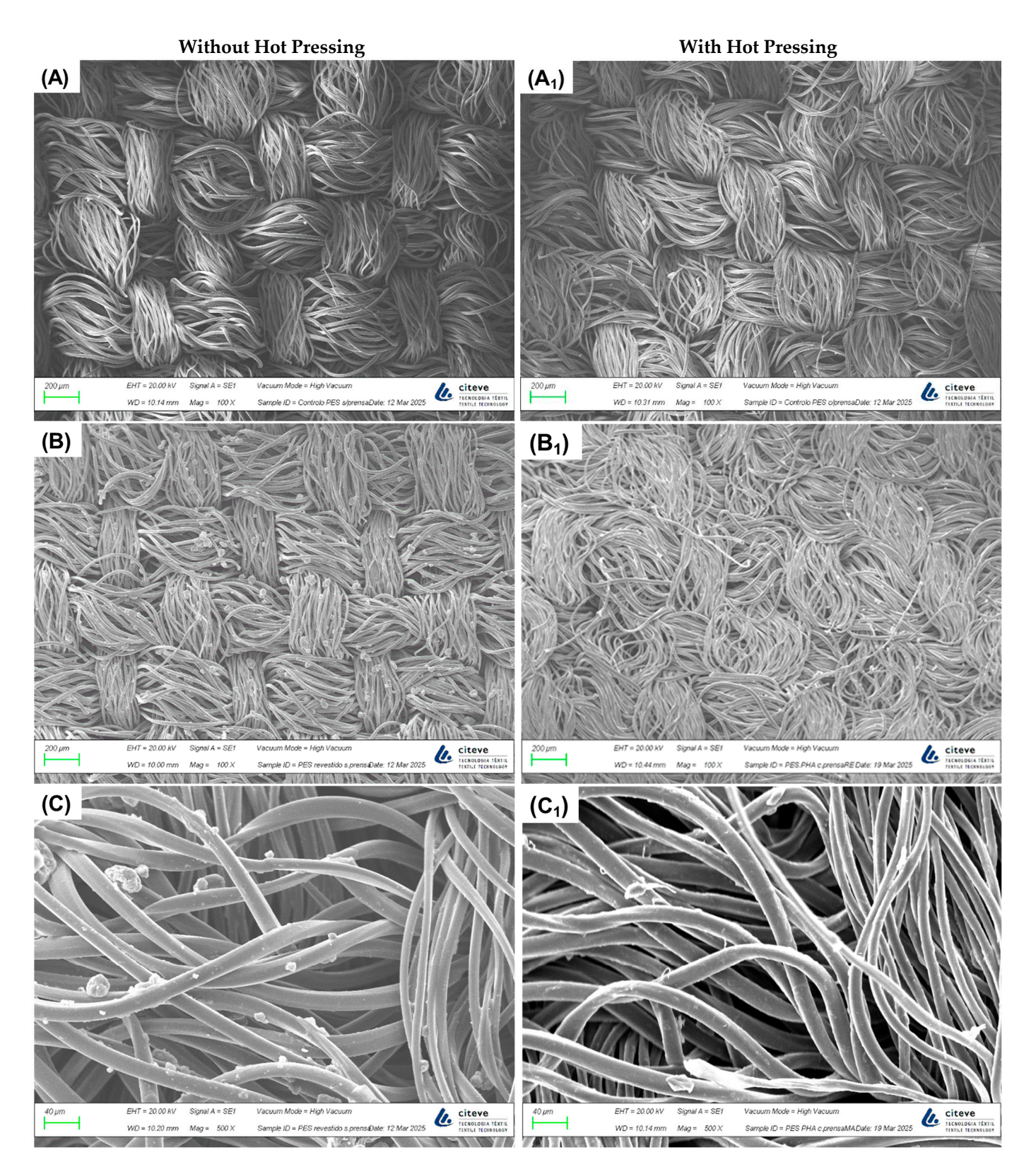


Figure 1. Cont.

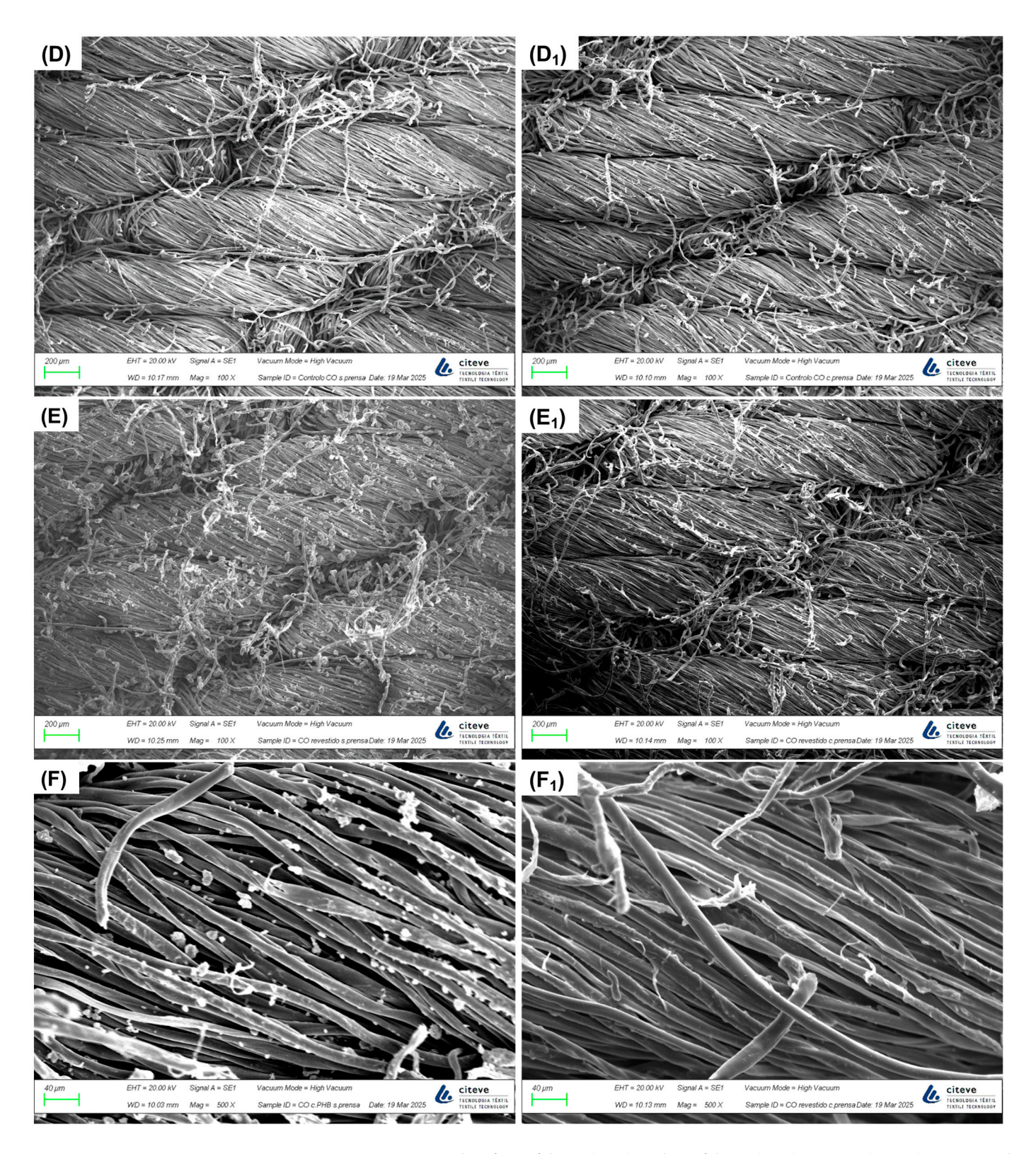


Figure 1. SEM micrographs of PES fabrics (**A–C**) and CO fabrics (**D–F**). Images (\mathbf{A}_1 – \mathbf{F}_1) correspond to the same substrates after undergoing the hot pressing process (180 °C). Images ($\mathbf{A}, \mathbf{B}, \mathbf{D}, \mathbf{E}$) were captured at 100× magnification, while images (\mathbf{C}, \mathbf{F}) were captured at 500× magnification.

Coatings 2025, 15, 1237 10 of 18

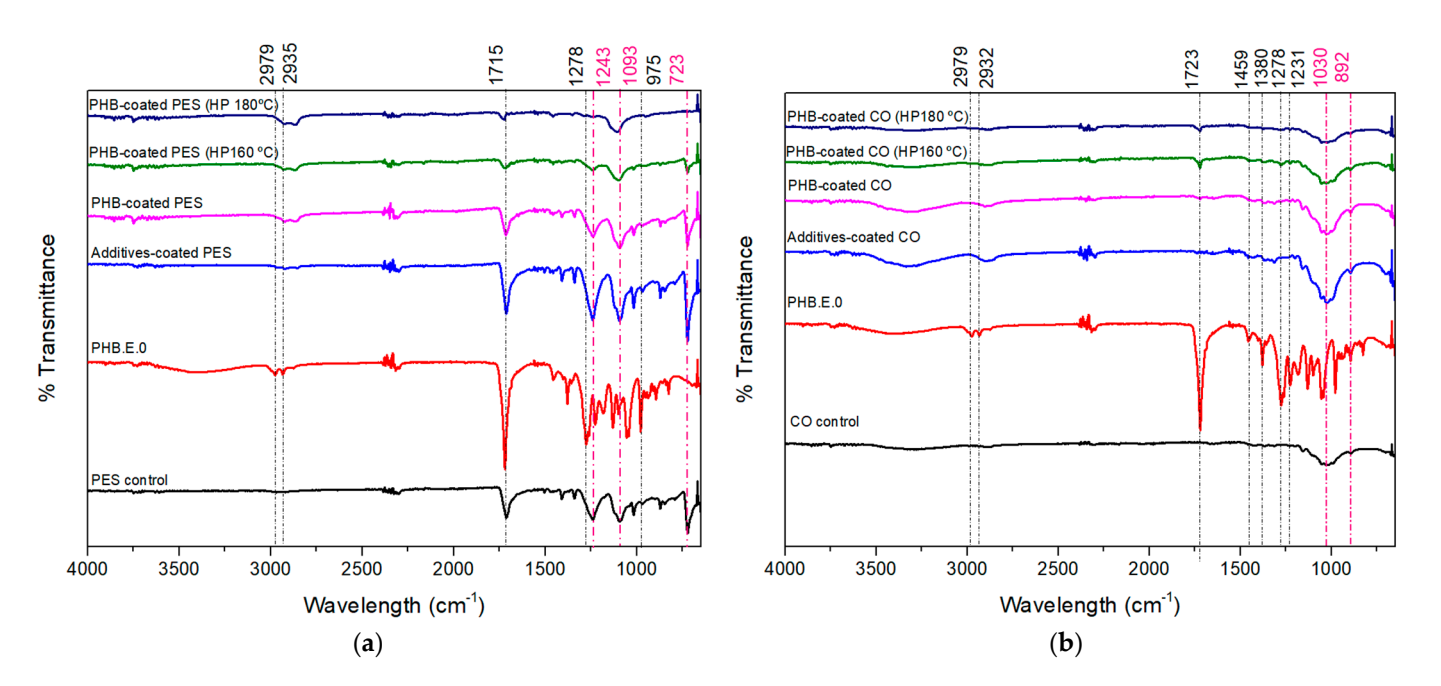


Figure 2. ATR-FTIR characterization of the textile substrates, the PHB.E.0 polymer, and the PHB.E.0-coated substrates, both unpressed and hot pressed (HP) at 160 °C and 180 °C. (a) FTIR spectra related to the modification of PES, and (b) FTIR spectra related to the modification of CO. The black dashed lines indicate bands characteristic of PHB.E.0, observed both in its pure spectrum and in the spectra of the PHB.E.0-coated substrates. In contrast, the pink dashed lines highlight the characteristic bands of each substrate.

The spectrum of PHB.E.0 powder exhibits the characteristic bands of PHAs, confirming the chemical identity of the synthesized polymer. The most prominent absorption band appears at $\approx 1720-1723~\rm cm^{-1}$, corresponding to the C=O stretching vibration of the ester carbonyl group, a primary fingerprint for the aliphatic polyester backbone of PHAs [30,31]. In addition, well-defined bands are observed at $\approx 2931~\rm cm^{-1}$ and $\approx 2876~\rm cm^{-1}$, attributed to the asymmetric and symmetric stretching vibrations of CH₃ and CH₂ groups, respectively, from the alkyl side chains. A set of bands between 1000 and 1300 cm⁻¹, particularly at 1276 cm⁻¹, are assigned to C–O–C stretching and CH bending, further supporting the presence of ester linkages and methylene groups. Additional bands at 1457 cm⁻¹ and 1380 cm⁻¹ are due to CH₂ scissoring and CH₃ symmetric bending, respectively, features typical of semi-crystalline PHAs [30–32].

In the PHB.E.0-coated PES fabrics, the PHA-related bands at \approx 2935 cm⁻¹ and \approx 2979 cm⁻¹ remain clearly visible, which may contribute to confirming the presence of the polymer on the synthetic substrate (Figure 2a). In the case of PHB.E.0-coated CO fabrics, the presence of the polymer is indicated by the band at around 1723 cm⁻¹, a characteristic feature of PHB.E.0. The observed shifts in the bands around 2932 and 2979 cm⁻¹ may reflect substrate-dependent interactions: on PES, which contains mainly ester groups and fewer hydrogen-bond-donating sites, interactions with PHB.E.0 are likely limited to weaker dipole–dipole or van der Waals forces; in contrast, on CO, the abundance of hydroxyl groups in cellulose can form stronger hydrogen bonds with the polymer's ester groups. These interactions can influence the vibrational energies of the C–H stretching modes, resulting in the small but measurable shifts observed in the ATR-FTIR spectra. Therefore, FTIR analysis confirms the chemical identity of the PES and CO substrates and the PHB.E.0 polymer, as well as the successful deposition of the coating on both textile surfaces, evidenced by the presence and persistence of characteristic PHB.E.0 absorption bands and substrate-dependent band shifts in the coated samples.

Coatings 2025, 15, 1237 11 of 18

3.4. TGA Analysis

TGA was conducted to evaluate the presence of PHB.E.0 on the fabrics and to assess the impact of the coating on the thermal properties of the treated textiles. It was performed on neat PHB.E.0 powder, uncoated textile substrates (CO and PES), and on PHB.E.0-coated substrates both without hot pressing and after being subjected to hot pressing at 160 °C and 180 °C. The TGA and corresponding derivative thermogravimetric (DTG) curves, carried out to identify the temperature ranges corresponding to the most prominent degradation events, are presented in Figures S1 and S2 (in Support Information), and the numerical results for onset temperature, maximum degradation temperature (T_d), and weight loss are summarized in Table 1. The degradation profiles revealed three main stages: an initial step, observed exclusively in cotton-based samples, related to the evaporation of adsorbed and absorbed moisture; a second step, attributed to the degradation of the PHB.E.0 coating; and a third step, corresponding to the thermal decomposition of the textile substrates themselves. The neat P3HB diol (PHB.E.0) exhibited a single-stage thermal degradation process, initiating at approximately 283.4 \pm 3.4 °C with a weight loss of about 97.7%.

The onset temperature of the PHB.E.0 layer varied depending on the substrate, indicating that the textile substrate plays a role in modulating the thermal behaviour of the coating. Specifically, the onset temperature was lower for PES (238.7 \pm 8.8 °C) compared to CO (252.2 \pm 11.3 °C), despite PES exhibiting a much higher thermal degradation temperature (421.0 \pm 1.6 °C) and greater residual mass than CO (354.3 \pm 1.7 °C). This discrepancy suggests that CO provides a more thermally protective and compatible interface for PHB.E.O. The improved performance on CO may be related to the porous and fibrous morphology of the CO substrates, which can facilitate more uniform anchoring of the coating, while their degradation behaviour may promote the formation of a char barrier that thermally shields the PHB.E.0 layer. The influence of hot pressing was also substrate dependent. On coated CO substrates, the onset temperature of PHB.E.0 increased with pressing temperature, rising from 252.2 °C (no pressing) to 254.5 °C and 259.1 °C at 160 °C and 180 °C respectively, likely due to improved hydrogen bonding or physical entanglement under heat and pressure, resulting in a more compact and stable interface. However, on coated PES substrates, the onset temperature decreased from 238.7 °C (no pressing) to 229.1 °C and 219.6 °C following hot pressing at 160 °C and 180 °C respectively, suggesting that thermal treatment may induce unfavourable morphological changes or weaken the adhesion between the PHB.E.0 coating and the PES substrate. Although PES exhibits inherently high thermal stability at its core, the observed interfacial degradation of the PHB.E.0 layer under these conditions indicates limited compatibility between the coating and substrate, resulting in a reduced protective effect. The relative weight loss attributed to the PHB.E.0 coating ranged from 1.3% to 1.8%, which is in close agreement with the initial polymer loading of 2%. This loss is primarily reflected in step 2 of the TGA curves presented in Table 2 and corresponds to the initial drop observed in Figure S3 to both PES and CO substrates (Supplementary Information). These results indicate that the majority of the applied polymer was effectively retained on the textile substrates, with only minimal loss during processing. Importantly, even this slight reduction highlights the establishment of interfacial interactions between the polymeric layer and the textile fibres, underscoring the effectiveness of the coating process.

Table 1. TGA thermal	parameters during	degradation	of PES and CO	fabrics.

		Step 1			Step 2			Step 3	
Samples	Onset Temp (°C)	T _d (°C)	Weigh Loss (%)	Onset Temp (°C)	T _d (°C)	Weigh Loss (%)	Onset Temp (°C)	T _d (°C)	Weigh Loss (%)
PHB.E.0	-	-	-	283.4 ± 3.4	309.6 ± 0.06	97.7 ± 0.7	-	-	-
PES control	-	-	-	-	-	-	421.0 ± 1.6	445.3 ± 0.23	81.8 ± 0.3
PHB.E.0- coated PES	-	-	-	238.7 ± 8.8	249.7 ± 1.6	1.8 ± 0.1	417.8 ± 1.0	445.2 ± 0.1	80.8 ± 0.7
PHB.E.0- coated PES	-	-	-	229.1 ± 10.6	244.8 ± 0.7	1.7 ± 0.1	417.0 ± 1.4	445.8 ± 0.2	81.3 ± 0.3
(160 °C) PHB.E.0-									
coated PES (180°C)	-	-	-	219.6 ± 4.0	246.5 ± 0.6	1.4 ± 0.2	418.0 ± 0.7	444.3 ± 0.3	80.7 ± 0.3
CO control	37.7 ± 11.4	67.9 ± 1.2	3.6 ± 0.3	-	-	-	354.3 ± 1.7	377.5 ± 1.6	89.8 ± 0.3
PHB.E.0- coated CO	36.7 ± 10.0	68.7 ± 4.7	3.0 ± 0.3	252.2 ± 11.3	-	1.3 ± 0.2	355.6 ± 1.2	381.1 ± 2.0	90.5 ± 0.8
PHB.E.0- coated CO (160°C)	29.6 ± 0.1	67.8 ± 1.5	2.6 ± 0.2	254.5 ± 9.0	-	1.7 ± 0.2	352.9 ± 0.9	383.4 ± 0.4	90.2 ± 0.4
PHB.E.0- coated CO (180 °C)	29.8 ± 0.1	68.5 ± 0.62	3.1 ± 0.3	259.1 ± 5.1	266.5 ± 2.3	1.8 ± 0.1	354.9 ± 0.6	380.5 ± 1.5	90.4 ± 0.4

T_d: Main thermal degradation temperature.

Table 2. Contact angles of PES and CO control fabrics, and PES and CO fabrics coated with PHB.E.0.

Sample		Treatment	Contact Angle (°) \pm S.D.	
PES	Control	Original fabric Hot Pressing (160°C) Hot Pressing (180°C) Surfactant/dispersant	$63.93 \pm 18.01 \\ 50.30 \pm 1.20 \\ 86.96 \pm 2.96 \\ \text{Absorbs instantly}$	
_	PHB.E.0 coating	Without hot pressing Hot Pressing (160 °C) Hot Pressing (180 °C)	Absorbs instantly Absorbs instantly 49.73 ± 7.87	
CO -	Control	Original fabric Surfactant/dispersant	Absorbs instantly	
	PHB.E.0 coating	Without hot pressing Hot Pressing (160 °C) Hot Pressing (180 °C)		

3.5. Wettability Analysis

Static contact angle measurements were performed to evaluate the surface wettability of the fabrics both before (controls) and after PHB.E.0 coating, as well as to investigate the impact of varying hot pressing temperatures on this property (Table 3). As PHAs are well known for their intrinsic hydrophobicity, it would be expected that the coated textiles would be more repellent to water than the uncoated textiles [33]. However, under all tested conditions, the fabrics consistently exhibited hydrophilic behaviour, likely due to the low concentration of PHB.E.0 in the formulation and the high content of hydrophilic additives.

Control PES fabrics not subjected to hot pressing exhibited a moderate contact angle of 63.93°, indicative of partial surface wettability. Hot pressing at 160 °C enhanced the surface hydrophilicity, as evidenced by a reduced contact angle of 50.30°. In contrast, increasing the temperature to 180 °C resulted in a rise in the contact angle to 86.96°, indicating decreased wettability. This reduction may be attributed to thermal restructuring or surface smoothing of the thermoplastic PES fabric induced specifically at 180 °C, which likely altered its surface energy. A similar effect was reported in the study developed by Oh et al. [34], where thermal treatment altered the surface properties leading to increased hydrophobicity. However, control samples treated only with surfactant and dispersant, without polymer,

demonstrated immediate drop absorption. Tween 80, a non-ionic surfactant, and Disperbyk 190, a polymeric dispersing agent, both contain hydrophilic groups that strongly interact with water molecules, promoting rapid water adsorption on the fabric surface [35]. PHB.E.0-coated PES samples exhibited immediate water absorption under all tested conditions, except after hot pressing at 180 °C, where a measurable contact angle of 49.73° was recorded, indicating the surface remained hydrophilic, although less than in the other conditions. The increase in contact angle observed after hot pressing at 180 °C is likely attributed to subtle surface modifications of the PES fabric induced by the thermal treatment, as supported by TGA analysis (with the lowest onset temperature) and consistent with trends noted in the uncoated control samples. The immediate water absorption observed in coated samples, both untreated and hot pressed at 160 °C, is likely due to the low concentration of PHB.E.0, its diol nature with available hydroxyl groups, and the presence of hydrophilic additives in the formulation. Overall, the results suggest that at the applied concentration, the PHB.E.0 coating did not significantly alter the surface energy nor confer hydrophobic character to the fabric.

Air Permeability Sample WVP (g·m $^{-2}$ ·24 h $^{-1}$) \pm S.D. I (%) \pm S.D. $(L \cdot m^{-2} \cdot s^{-1}) \pm S.D.$ 670.0 ± 8.7 Original fabric 574.9 ± 9.4 96.3 ± 9.4 Hot Pressing (160 °C) Control Hot Pressing (180 °C) 128.1 ± 9.9 568.0 ± 1.6 95.3 ± 1.6 PES Surfactant/dispersant 346.0 ± 4.5 574.7 ± 4.1 97.0 ± 4.1 Without hot pressing 344.0 ± 4.8 569.7 ± 4.7 95.3 ± 5.7 PHB.E.0 coating Hot Pressing (160 °C) Hot Pressing (180 °C) 171.0 ± 28.4 563.0 ± 4.2 94.5 ± 4.2 Original fabric 50.2 ± 2.4 571.4 ± 6.0 94.0 ± 6.0 Control 559.5 ± 5.5 Surfactant/dispersant 38.5 ± 2.4 94.0 ± 5.5 CO Without hot pressing 31.6 ± 3.8 558.2 ± 1.1 92.0 ± 1.1

 29.8 ± 3.1

Table 3. Air and water vapor permeability.

Regarding CO fabrics, inherently hydrophilic, exhibited immediate water absorption across all control and PHB.E.0-coated samples, irrespective of the hot pressing temperature. This behaviour confirms that the surface properties of cotton remained unaffected, consistent with its strong natural affinity for water. Unlike PES, cotton control fabrics were not subjected to hot pressing, as cotton is not a thermoplastic polymer. Additionally, the concentration of PHB.E.0 applied was insufficient to significantly modify surface energy or impart hydrophobicity to cotton, paralleling the findings observed for PES fabrics.

 577.6 ± 13.6

 93.0 ± 13.6

3.6. Water Absorption Test

Hot Pressing (160 °C)
Hot Pressing (180 °C)

PHB.E.0 coating

The water absorption capacity of fibres is a critical factor influencing the thermal comfort of sportswear by facilitating moisture management and aiding in body temperature regulation through sweat wicking; therefore, this property was evaluated alongside contact angle measurements [36]. Water absorption data complemented contact angle analysis to provide a comprehensive understanding of fabric wettability and moisture-handling behaviour. All water absorption values for the samples are shown in Figure 3.

In uncoated PES fabrics, a clear correlation between contact angle and water absorption was observed. Application of hot pressing at $180\,^{\circ}\text{C}$ significantly reduced water absorption from 78.9% to 66.8%, concomitant with a slight increase in contact angle, in-

Coatings 2025, 15, 1237 14 of 18

dicating decreased surface wettability. Samples treated solely with additives exhibited water absorption values comparable to untreated PES, suggesting that despite rendering the surface highly hydrophilic (as evidenced by the absence of a measurable contact angle), additives alone did not enhance water uptake within the substrate structure. Similarly, PHB.E.0-coated PES fabrics showed negligible variation in water absorption, consistent with contact angles remaining within the hydrophilic regime. Notably, all PES samples required more than 180 s to sink in this water absorption test, highlighting that the applied coatings and treatments had minimal effect on the overall sinking behavior. The observed reduction in water absorption following hot pressing is attributed primarily to surface morphology alterations arising from the thermoplastic nature of PES, as corroborated by TGA analysis, rather than from the polymer coating itself. Consequently, PHB.E.0 coatings at the applied concentration exert minimal influence on the water absorption of PES substrates. In contrast, uncoated CO fabrics that did not undergo hot pressing displayed slightly higher water absorption (≈66%) relative to those subjected to thermal treatment (\approx 59%). This decrease is likely attributable to increased fibre densification induced by the hot pressing process, as supported by SEM micrographs (Figure 1). Notably, CO fabrics hot pressed at 160 °C and 180 °C exhibited comparable water absorption levels, suggesting that once fiber compaction is achieved, further increases in pressing temperature have a limited effect on moisture uptake. For CO fabrics coated with PHB.E.O, a modest reduction in water absorption was observed compared to their uncoated counterparts, likely due to the polymer coating partially masking cotton's intrinsic hydrophilicity and abundant hydroxyl groups. Among these coated samples, those hot pressed at 180 °C showed the lowest water absorption (\approx 54%), which may be attributed to enhanced interfacial interactions between PHB.E.0 and the substrate facilitated by this temperature, as supported by TGA results. It is noteworthy that CO samples sank immediately upon being placed on the water surface, reflecting the highly hydrophilic and porous nature of cellulose fabrics. Collectively, these findings indicate that the PHB.E.0 coating alone exerts a limited effect on the water absorption properties of both PES and CO substrates, with hot pressing additionally influencing surface wettability.

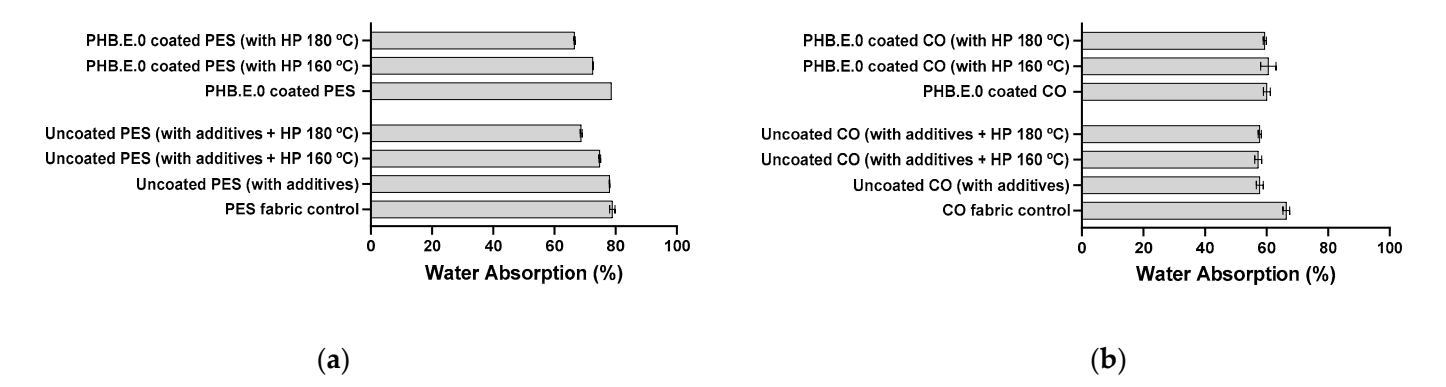


Figure 3. Water absorption values (%) of (a) PES fabric control (uncoated PES) and PHB.E.0 coated PES; (b) CO fabric control (uncoated CO) and PHB.E.0 coated CO.

3.7. Permeabilities

Both air permeability and WVP are critical metrics to evaluate textile breathability, as they directly regulate the exchange of heat and moisture vapor between the skin and the ambient environment. Efficient breathability facilitates sweat evaporation through the fabric, thereby maintaining skin dryness and overall thermal comfort for the wearer [34]. To elucidate the effects of PHB.E.0 coating and hot pressing treatment on the breathability of the PES and CO fabrics, comprehensive air and WVP assessments were conducted (Table 3).

Coatings 2025, 15, 1237 15 of 18

For PES substrates, the untreated control fabrics (original fabrics) exhibited high air permeability (670.0 L m⁻²·s⁻¹) alongside substantial WVP (574.9 g·m⁻²·24 h⁻¹), reflecting its inherently porous and breathable structure. Hot pressing at 180 °C of these uncoated PES substrates caused a substantial reduction in air permeability by approximately 81% (down to $128.0 \text{ L} \cdot \text{m}^{-2} \cdot \text{s}^{-1}$), while WVP slight decreased (568.0 g·m⁻²·24 h⁻¹). The pronounced decline in air permeability is attributed to thermally induced densification and surface restructuring, characteristic of the thermoplastic behavior of PES, as confirmed by SEM morphological analysis and TGA observations. During hot pressing, the PES fibers partially soften and rearrange, leading to compaction of the textile structure. This reduces pore size and inter-fiber spacing, significantly restricting convective airflow while largely preserving pathways for vapor diffusion. Consequently, the fabric retains its ability to transport moisture vapor despite the notable reduction in air exchange. In relation to treatment exclusively with surfactant and dispersant additives, a significant reduction (pprox48%) in air permeability was observed (346 $L \cdot m^{-2} \cdot s^{-1}$), without significantly impacting water vapor permeability. These findings suggest that the application of additives contributes to altering the fabric's physical porosity without affecting its capacity for vapor transmission. Similarly, applying the PHB.E.0 coating without subsequent thermal treatment led to a significant reduction in air permeability (\approx 49%, 344.0 L·m⁻²·s⁻¹) compared to the untreated control fabric. In contrast, WVP was only marginally affected (\approx 1%), indicating that the concentration of PHA applied was relatively low. Although PHAs are inherently hydrophobic and typically serve as effective barriers to water vapor, the results observed were comparable to those of the uncoated samples [17].

However, it is important to note that the air permeability of PHB.E.0-coated PES did not differ significantly from that of the PES substrate modified solely with additives, suggesting that the polymer had limited influence on this parameter. When PHB.E.0-coated PES fabrics were hot pressed at 180 °C, air permeability further decreased to 171.0 $\rm L\cdot m^{-2}\cdot s^{-1}$, representing a 74% reduction compared to the untreated control, accompanied by a slight decrease in WVP (564.0 g·m $^{-2}\cdot 24$ h $^{-1}$). However, comparing PHB.E.0-coated PES fabrics hot pressed at 180 °C to those not hot pressed, air permeability was reduced by approximately 50%, while the change in WVP remained insignificant. These findings emphasize that the thermal treatment is the primary factor influencing permeability, particularly air permeability, under these conditions.

In contrast, CO fabrics naturally exhibited significantly lower air permeability (50.2 L·m $^{-2}$ ·s $^{-1}$) due to their denser fibrous structure (higher grammage), while maintaining a WVP (571.4 g·m $^{-2}$ ·24 h $^{-1}$) comparable to that of PES samples. Treatment with additives and PHB.E.0 coating further reduced air permeability to approximately 32–39 L·m $^{-2}$ ·s $^{-1}$, representing decreases of 23% and 37%, respectively, with negligible effects on vapor permeability. Notably, PHB.E.0-coated CO fabrics subjected to hot pressing at 180 °C exhibited the lowest air permeability (29.8 L·m $^{-2}$ ·s $^{-1}$), corresponding to a 40% reduction relative to untreated control CO fabrics, alongside a slight increase in WVP (577.6 g·m $^{-2}$ ·24 h $^{-1}$). This indicates that thermal compaction restricts convective airflow but may enhance microstructural pathways that favour vapor diffusion. This nuanced behaviour in CO fabrics highlights the complex interplay between natural fibre morphology and thermal processing.

Across all treatments, the WVP index (I%) of the PHB.E.0-coated fabrics remained consistently high ($\approx\!92\text{--}97\%$), confirming their effective moisture regulation. Hot pressing further reduced air permeability, enhancing structural integrity and wind resistance without compromising breathability. In comparison, commercial GORE-TEX® fabrics, such as the Pro 2-Layer and 3-Layer (25,000 g·m $^{-2}\cdot24$ h $^{-1}$), Performance Shell (17,000 g·m $^{-2}\cdot24$ h $^{-1}$), and Paclite (15,000 g·m $^{-2}\cdot24$ h $^{-1}$), exhibit extremely low air permeability ($\approx\!28$ L/min/m 2)

Coatings 2025, 15, 1237 16 of 18

and high moisture vapor permeability (as indicated by the MVTR values above), reflecting their superior windproofing and breathability performance. These differences are largely due to the multi-layered structure of GORE-TEX®, which combines a porous ePTFE membrane with outer and inner fabrics to provide waterproofing, windproofing, and controlled moisture transport. In contrast, our approach employs a single biopolymer coating applied via a spray method, offering a sustainable and versatile alternative for modifying different substrates. While PHB.E.O-coated textiles do not yet match commercial standards, they demonstrate a promising balance between reduced air permeability and maintained vapor transport, highlighting their potential for applications requiring moderate breathability and moisture management. These findings provide a benchmark for the performance gap between conventional, fossil-based membranes and the developed biopolymer coatings, guiding future optimization and structural or hybrid improvements for outdoor textile applications.

4. Conclusions

This study demonstrates the successful development and application of a sustainable coating system based on chemically modified poly(3-hydroxybutyrate)-diol (PHB.E.0), formulated as an aqueous dispersion and applied to PES and CO fabrics via a solvent-free spray-coating technique. The coating process was confirmed through morphological, chemical, and thermal analyses, including SEM, ATR-FTIR, elemental analysis, and TGA.

Despite the addition of the biopolymer layer and subsequent thermal treatment, the coated textiles retained their hydrophilic character, facilitating moisture uptake and transfer, while maintaining high water vapor permeability, essential for breathability. At the same time, a significant reduction in air permeability was achieved, particularly in hot pressed samples, indicating improved wind resistance. These enhancements were achieved without compromising vapor transport, reflecting a well-balanced improvement in textile functionality.

This work serves therefore as a first step toward understanding the interactions between PHB.E.0 and both synthetic and natural fibre substrates. TGA results highlight substrate-dependent thermal behaviour and suggest complex interfacial phenomena that merit further investigation. Given the intrinsic challenges in achieving strong interfacial adhesion between hydrophobic PHA and hydrophilic fibres, especially under mechanical or washing conditions, future work may be focused on evaluating adhesion performance and exploring strategies such as surface modification or compatibilizer incorporation to strengthen the polymer–substrate interface. Furthermore, the effect of increasing PHB.E.0 concentration on coating performance may be systematically explored to determine the optimal balance between coating thickness, durability, and breathability. Insights from these studies would inform the development of optimized, scalable formulations.

Overall, PHB.E.0 coatings offer a promising and environmentally responsible pathway for enhancing textile performance, contributing to the advancement of sustainable, high-performance materials for sportswear and technical apparel.

Supplementary Materials: The following supporting information can be downloaded at: https://www.mdpi.com/article/10.3390/coatings15111237/s1, Figure S1. Gel permeation chromatography (GPC) chromatogram of PHB.E.0, showing the polymer's retention time and distribution. Figure S2. Size distribution by intensity of the PHB.E.0 dispersion as determined by DLS. Figure S3. Zeta potential distribution of the PHB.E.0 dispersion. Figure S4. Thermogravimetric analysis (TGA) of (a) PES substrates and PHB.E.0-coated PES; (b) CO substrates and PHB.E.0-coated CO. Images (a₁) and (b₁) present magnified views of the initial degradation regions for PES and CO substrates, respectively. Figure S5. Derivative thermogravimetric analysis (DTG) of (a) PES substrates

Coatings **2025**, 15, 1237 17 of 18

and PHB.E.0-coated PES substrates, with the corresponding magnified view shown in (a_1) ; (b) CO substrates and PHB.E.0-coated CO samples.

Author Contributions: M.A.T.: Conceptualization, Investigation, Methodology, Writing—original draft; W.A.: Investigation, Methodology, Writing—original draft; J.C.: Investigation, Methodology; C.G.: Review & editing, Supervision; H.V.: Review & editing, Supervision, Project administration; C.J.S.: Supervision, Project administration. All authors have read and agreed to the published version of the manuscript.

Funding: This work was carried out under the Horizon Europe 2021–2027 programme (project Waste2BioComp, Grant Agreement 101058654), funded under the topic HORIZON-CL4-2021-TWINTRANSITION-01-05 of the Horizon Europe 2021–2027 programme.

Institutional Review Board Statement: Not applicable.

Informed Consent Statement: Not applicable.

Data Availability Statement: The data that support the findings of this study are available from the corresponding author upon reasonable request.

Acknowledgments: The authors sincerely thank the Waste2BioComp project for making the development of this research possible.

Conflicts of Interest: The authors declare no conflicts of interest related to this study. No financial or personal relationships exist that could have inappropriately influenced the results or interpretation of the research.

References

- 1. Tang, K.H.D. Advances in Thermoregulating Textiles: Materials, Mechanisms, and Applications. Textiles 2025, 5, 22. [CrossRef]
- 2. Islam, M.R.; Golovin, K.; Dolez, P.I. Clothing Thermophysiological Comfort: A Textile Science Perspective. *Textiles* **2023**, *3*, 353–407. [CrossRef]
- 3. Adámek, K.; Havelka, A.; Kůs, Z.; Mazari, A. Correlation of Air Permeability to Other Breathability Parameters of Textiles. *Polymers* **2021**, *14*, 140. [CrossRef]
- 4. Pradhan, L.; Maiti, S.; Mallick, A.; Shahid, M.; More, S.P.; Adivarekar, R.V. 3 Coating- and Lamination-Based Smart Textiles: Techniques, Features, and Challenges. In *Smart and Functional Textiles*; De Gruyter: Berlin, Germany, 2023; pp. 97–150. [CrossRef]
- 5. Cui, G.; Wang, C. Applications and Development Trends of Textile Materials in Sports: A Review. *Alex. Eng. J.* **2025**, *126*, 491–506. [CrossRef]
- 6. Sfameni, S.; Lawnick, T.; Rando, G.; Visco, A.; Textor, T.; Plutino, M.R. Super-Hydrophobicity of Polyester Fabrics Driven by Functional Sustainable Fluorine-Free Silane-Based Coatings. *Gels* **2023**, *9*, 109. [CrossRef]
- 7. Kim, H.-A. Water Repellency/Proof/Vapor Permeability Characteristics of Coated and Laminated Breathable Fabrics for Outdoor Clothing. *Coatings* **2021**, *12*, 12. [CrossRef]
- 8. Ullah, H.M.K.; Lejeune, J.; Cayla, A.; Monceaux, M.; Campagne, C.; Devaux, É. A Review of Noteworthy/Major Innovations in Wearable Clothing for Thermal and Moisture Management from Material to Fabric Structure. *Text. Res. J.* **2022**, *92*, 3351–3386. [CrossRef]
- 9. Taliantzis, K.; Ellinas, K. Green Hydrophobic and Superhydrophobic Coatings and Surfaces for Water Related Applications: A Review. *Adv. Colloid Interface Sci.* **2025**, 343, 103566. [CrossRef] [PubMed]
- 10. Schellenberger, S.; Hill, P.J.; Levenstam, O.; Gillgard, P.; Cousins, I.T.; Taylor, M.; Blackburn, R.S. Highly Fluorinated Chemicals in Functional Textiles Can Be Replaced by Re-Evaluating Liquid Repellency and End-User Requirements. *J. Clean. Prod.* **2019**, 217, 134–143. [CrossRef]
- 11. Khan, M.F. Recent Progress and Challenges in Microbial Defluorination and Degradation for Sustainable Remediation of Fluorinated Xenobiotics. *Processes* **2025**, *13*, 2017. [CrossRef]
- Lukić Bilela, L.; Matijošytė, I.; Krutkevičius, J.; Alexandrino, D.A.M.; Safarik, I.; Burlakovs, J.; Gaudêncio, S.P.; Carvalho, M.F. Impact of Per- and Polyfluorinated Alkyl Substances (PFAS) on the Marine Environment: Raising Awareness, Challenges, Legislation, and Mitigation Approaches under the One Health Concept. Mar. Pollut. Bull. 2023, 194, 115309. [CrossRef] [PubMed]
- 13. Polo Fonseca, L.; Duval, A.; Luna, E.; Ximenis, M.; De Meester, S.; Avérous, L.; Sardon, H. Reducing the Carbon Footprint of Polyurethanes by Chemical and Biological Depolymerization: Fact or Fiction? *Curr. Opin. Green Sustain. Chem.* **2023**, *41*, 100802. [CrossRef]

Coatings 2025, 15, 1237 18 of 18

14. Ali, A.; Qamer, S.; Shahid, M.; Tomkova, B.; Khan, M.Z.; Militky, J.; Wiener, J.; Venkataraman, M. Micro- and Nanoplastics Produced from Textile Finishes: A Review. *Langmuir* **2024**, *40*, 17849–17867. [CrossRef]

- 15. Pradhan, S.; Khan, M.T.; Moholkar, V.S. Polyhydroxyalkanoates (PHAs): Mechanistic Insights and Contributions to Sustainable Practices. *Encyclopedia* **2024**, *4*, 1933–1947. [CrossRef]
- 16. Mai, J.; Kockler, K.; Parisi, E.; Chan, C.M.; Pratt, S.; Laycock, B. Synthesis and Physical Properties of Polyhydroxyalkanoate (PHA)-Based Block Copolymers: A Review. *Int. J. Biol. Macromol.* **2024**, 263, 130204. [CrossRef]
- 17. Jahangiri, F.; Mohanty, A.K.; Misra, M. Sustainable Biodegradable Coatings for Food Packaging: Challenges and Opportunities. *Green Chem.* **2024**, 26, 4934–4974. [CrossRef]
- 18. Kunam, P.K.; Ramakanth, D.; Akhila, K.; Gaikwad, K.K. Bio-Based Materials for Barrier Coatings on Paper Packaging. *Biomass Convers. Biorefinery* **2024**, 14, 12637–12652. [CrossRef] [PubMed]
- 19. Gundlapalli, M.; Ganesan, S. Polyhydroxyalkanoates (PHAs): Key Challenges in Production and Sustainable Strategies for Cost Reduction within a Circular Economy Framework. *Results Eng.* **2025**, *26*, 105345. [CrossRef]
- Uddin, M.K.; Novembre, L.; Greco, A.; Sannino, A. Polyhydroxyalkanoates, A Prospective Solution in the Textile Industry—A Review. Polym. Degrad. Stab. 2024, 219, 110619. [CrossRef]
- German Institutes of Textile and Fiber Research Denkendorf. Coating with Polyhydroxyalkanoates: Biopolymers from Bacteria Protect Technical Textiles. Press Release, 22 February 2024.
- 22. Shahid, M.A.; Rahman, M.M.; Hossain, M.T.; Hossain, I.; Sheikh, M.S.; Rahman, M.S.; Uddin, N.; Donne, S.W.; Hoque, M.I.U. Advances in Conductive Polymer-Based Flexible Electronics for Multifunctional Applications. *J. Compos. Sci.* **2025**, *9*, 42. [CrossRef]
- 23. Ghosh, J.; Rupanty, N.S.; Noor, T.; Asif, T.R.; Islam, T.; Reukov, V. Functional Coatings for Textiles: Advancements in Flame Resistance, Antimicrobial Defense, and Self-Cleaning Performance. *RSC Adv.* **2025**, *15*, 10984–11022. [CrossRef] [PubMed]
- 24. Trabucco, S.; Ortelli, S.; Del Secco, B.; Zanoni, I.; Belosi, F.; Ravegnani, F.; Nicosia, A.; Blosi, M.; Costa, A.L. Monitoring and Optimisation of Ag Nanoparticle Spray-Coating on Textiles. *Nanomaterials* **2021**, *11*, 3165. [CrossRef] [PubMed]
- 25. Sasaki, K.; Tenjimbayashi, M.; Manabe, K.; Shiratori, S. Asymmetric Superhydrophobic/Superhydrophilic Cotton Fabrics Designed by Spraying Polymer and Nanoparticles. *ACS Appl. Mater. Interfaces* **2016**, *8*, 651–659. [CrossRef]
- 26. Gabardo, R.S.; de Carvalho Cotre, D.S.; Lis Arias, M.J.; Moisés, M.P.; Martins Ferreira, B.T.; Samulewski, R.B.; Hinestroza, J.P.; Bezerra, F.M. Surface Modification of Polyester Fabrics by Ozone and Its Effect on Coloration Using Disperse Dyes. *Materials* **2021**, *14*, 3492. [CrossRef]
- 27. Ebrahimi, I.; Kiumarsi, A.; Parvinzadeh Gashti, M.; Rashidian, R.; Hossein Norouzi, M. Atmospheric-Air Plasma Enhances Coating of Different Lubricating Agents on Polyester Fiber. *Eur. Phys. J. Appl. Phys.* **2011**, *56*, 10801. [CrossRef]
- 28. Zhang, L.; Li, X.; Zhang, S.; Gao, Q.; Lu, Q.; Peng, R.; Xu, P.; Shang, H.; Yuan, Y.; Zou, H. Micro-FTIR Combined with Curve Fitting Method to Study Cellulose Crystallinity of Developing Cotton Fibers. *Anal. Bioanal. Chem.* **2021**, *413*, 1313–1320. [CrossRef]
- 29. Kong, D.; Liu, J.; Zhang, Z.; Wang, S.; Lu, Z. Preparation of Synergistic Silicon, Phosphorus and Nitrogen Flame Retardant Based on Cyclosiloxane and Its Application to Cotton Fabric. *Cellulose* **2021**, *28*, 8115–8128. [CrossRef]
- 30. Julinová, M.; Šašinková, D.; Minařík, A.; Kaszonyiová, M.; Kalendová, A.; Kadlečková, M.; Fayyazbakhsh, A.; Koutný, M. Comprehensive Biodegradation Analysis of Chemically Modified Poly(3-Hydroxybutyrate) Materials with Different Crystal Structures. *Biomacromolecules* 2023, 24, 4939–4957. [CrossRef]
- 31. Ramezani, M.; Amoozegar, M.A.; Ventosa, A. Screening and Comparative Assay of Poly-Hydroxyalkanoates Produced by Bacteria Isolated from the Gavkhooni Wetland in Iran and Evaluation of Poly-β-Hydroxybutyrate Production by Halotolerant Bacterium *Oceanimonas* sp. GK1. *Ann. Microbiol.* **2015**, *65*, 517–526. [CrossRef]
- 32. Teixeira, M.A.; Leite, I.; Gonçalves, R.; Vilaça, H.; Guise, C.; Silva, C. Comprehensive Evaluation of Wet-Spun Polyhydroxyalkanoate Fibres: Morphology, Crystallinity, and Thermal Properties. *Fibers* **2025**, *13*, 111. [CrossRef]
- 33. Andreotti, S.; Franzoni, E.; Degli Esposti, M.; Fabbri, P. Poly(Hydroxyalkanoate)s-Based Hydrophobic Coatings for the Protection of Stone in Cultural Heritage. *Materials* **2018**, *11*, 165. [CrossRef] [PubMed]
- 34. Oh, J.-H.; Ko, T.-J.; Moon, M.-W.; Park, C.H. Nanostructured Fabric with Robust Superhydrophobicity Induced by a Thermal Hydrophobic Ageing Process. *RSC Adv.* **2017**, *7*, 25597–25604. [CrossRef]
- 35. Simončič, B.; Rozman, V. Wettability of Cotton Fabric by Aqueous Solutions of Surfactants with Different Structures. *Colloids Surf. A Physicochem. Eng. Asp.* **2007**, 292, 236–245. [CrossRef]
- 36. Manshahia, M.; Das, A. Moisture Management of High Active Sportswear. Fibers Polym. 2014, 15, 1221–1229. [CrossRef]

Disclaimer/Publisher's Note: The statements, opinions and data contained in all publications are solely those of the individual author(s) and contributor(s) and not of MDPI and/or the editor(s). MDPI and/or the editor(s) disclaim responsibility for any injury to people or property resulting from any ideas, methods, instructions or products referred to in the content.